THE JOURNAL OF PHYSICAL CHEMISTRY A

 VOLUME 104, NUMBER 30, AUGUST 3, 2000

ARTICLES

Ultrafast Excited State Dynamics of Oxidized Flavins: Direct Observations of Quenching by Purines

Robert J. Stanley* and Alexander W. MacFarlane IV

Department of Chemistry, Temple University, Philadelphia, Pennsylvania 19122

Received: January 4, 2000; In Final Form: May 8, 2000

We have measured the excited-state dynamics and spectral evolution of oxidized flavin−adenine dinucleotide (FAD_{ox}) and flavin mononucleotide (FMN_{ox}) in simple solvents with subpicosecond time resolution by one-color and white-light continuum transient absorption spectroscopy. In water, the FAD_{ox} transient shows significant quenching of the excited state with a lifetime of ~4 ps while for FMN_{ox} this component is of much lower amplitude. However, when caffeine is added to the FMN solution the amplitude of the fast component is recovered. Additionally, the excited-state dynamics of FAD in neat formamide, a solvent that breaks up stacking interactions in FAD, is similar to that obtained for FMN in water. These measurements provide conclusive evidence that the excited-state quenching observed in FAD or flavin−purine complexes occurs in less than 5 ps. The observed spectral evolution shows that internal conversion from S_2 to S_1 occurs in less than 100 fs.

Introduction

Flavins are heterocyclic molecules whose electronic properties allow them to serve as versatile electron donors and acceptors in a bewildering variety of biological roles.[1−4] As enzyme cofactors, they consist of an isoalloxazine moiety tethered to a ribtyl chain that can be substituted in a number of ways. Flavin mononucleotide (FMN), riboflavin, and flavin−adenine dinucleotide (FAD) are the most commonly occurring cofactors. Oxidized FMN and riboflavin in water have a large fluorescence quantum yield.[5] The lifetime for the lowest singlet excited state (S_1) of FMN and riboflavin is several nanoseconds; however the lifetime of the S_1 state can be reduced by interaction of the flavin with aromatic molecules such as tryptophan, tyrosine, and phenylalanine.[5−8] This excited-state quenching has been used to investigate protein−cofactor interactions in a variety of flavoproteins. The structural requirement for this kind of excited-state quenching appears to be the formation of a coplanar π-stacked complex.[9−12]

An example of this interaction is the coplanar stacking of isoalloxazine and adenine of flavin−adenine dinucleotide in water which has attracted considerable interest for more than 50 years.[5] The stacking interaction leads to a 10-fold decrease in the fluorescence quantum yield of oxidized FAD (FAD_{ox}) in aqueous solutions at neutral pH when compared to other flavins such as FMN_{ox}.[5] FAD is also known to undergo dynamic quenching in aqueous solution. Studies have shown that 80% of ground-state FAD molecules are in the stacked configuration at room temperature.[6] but that dynamic stacking and unstacking can occur with a rate of 1.9×10^8 s^{-1}. This process is slow relative to the time window utilized in the experiments reported below. However, this conformational inhomogeneity will lead to a broadened rate distribution for quenching (vide infra).

It is of considerable interest to understand how the electronic properties of the isoalloxazine heterocycle are modified when placed in communication with aromatic residues in and around the protein binding pocket. It is well established that these interactions are capable of tuning the redox potential of flavoproteins.[1,3,13] However, when electron transfer takes place

10.1021/jp000003y CCC: $19.00
Published on Web 07/01/2000

following the absorption of a photon, as is the case of the DNA repair protein DNA photolyase, it is the redox potential of the excited state that is relevant to the electron-transfer efficiency.[14] The free energy available for excited-state electron transfer (and therefore its rate) depends on the vibronic level from which this reaction takes place.[15] Thus, the relaxation dynamics of the excited electronic state become important, particularly when electron transfer occurs in the same time regime as vibronic relaxation.[16] In addition, when the flavin cofactor is strongly coupled to surrounding aromatic residues, then excited state electron transfer must compete effectively with internal conversion to the ground state. Interestingly, the conformation of FAD in photolyase is unique in that the adenine is in close proximity to the isoalloxazine ring. It is not known whether this stacked conformation plays a functional role in the protein, but it is unusual that the geometry appears to be different from that of all other flavoprotein crystal structures solved to date, none of which use light as a catalytic factor.

Given these kinetic considerations, a direct measurement of the rate of excited-state quenching would also be of value as a measure of the strength of this interaction as well as the orientation of the flavin relative to the residue responsible for this interaction. A number of studies aimed at elucidating the dynamics of the quenching process[6,8,12,17,18] did not unambiguously resolve the primary kinetics for this interaction. Recent fluorescence studies in flavoproteins with higher time resolution have shown that in the tightly packed protein environment the excited state of flavins are efficiently quenched in 7 ps or less.[19−21] A fluorescence upconversion study of riboflavin binding protein suggests that vibronically excited riboflavin undergoes vibrational relaxation in less than 100 fs when quenched by the protein matrix. In contrast, we have performed subpicosecond transient absorption measurements that provide direct evidence for the time scale of excited-state quenching of FAD and FMN−caffeine complexes in simple solvents. Additionally, our measurements set an upper limit on the rate of internal conversion from $S_2 \rightarrow S_1$. A preliminary account of this research has been presented earlier.[22]

Experimental Section

Subpicosecond Transient Absorption Spectrometer. The transient spectrometer has not been reported previously in detail. It consists of a 1 kHz Ti:sapphire regenerative amplifier (Positive Light Spitfire-LCX), pumped by a 7 W CW-Q-switched Nd:YLF laser (Positive Light Merlin). The regenerative amplifier is seeded by an 80 MHz Ti:sapphire mode-locked laser oscillator constructed from a kit (Kapteyn-Murnane) and pumped by an Ar^+ laser with ∼5 W, all lines (Spectra Physics 2060-7S). The Ti:S laser is capable of ca. 30 fs pulses but by narrowing an intracavity slit the pulses are broadened to about 80 fs. The slit also allows for tuning the wavelength of the laser from less than 750 nm to above 840 nm. The amplifier optics permit tuning from about 760 to 840 nm.

The fundamental was divided into photolysis and probe beams. The photolysis pulse was generated by frequency-doubling the fundamental in a 2 mm thick type I BBO crystal to produce UV light with ∼20% conversion efficiency. This gives a pulse with about 2 nm of bandwidth. One-color experiments were performed by splitting off a small fraction of the doubled light with an uncoated fused silica flat. The photolysis pulse is sent through a variable optical delay consisting of an Al-coated hollow retroreflector mounted on a motor-driven translation stage with a 3 ns range and a maximum resolution of about 8 fs (Aerotech). The beam is attenuated by one or two 1 mm thick fused-silica neutral density filters or absorptive filters and focused into a 0.5−2 mm path length glass or fused silica flow cell. A peristaltic pump is used to flow the sample solution at a rate sufficient to replace the sample for every photolysis pulse. Pump energies are ≤400 nJ/pulse. The absorbance change is linear with up to ∼5% photolysis, corresponding to $\Delta A \sim 30$ mOD for a 0.6 optical density (OD) sample absorbance.

For the white-light[23] continuum studies, the probe beam is generated by first focusing the fundamental into a 2 mm thick crystal quartz or sapphire flat using a plano convex lens (for one-color pump−probe experiments the optical flat was removed). Best results are obtained using a 20 cm focal length lens with the quartz flat though some data were taken with a continuum generated using a 5 cm focal length lens. The continuum is recollimated with a 90° off-axis aluminum parabola (Janos Technology). The probe pulse is subsequently divided into sample and reference beams using a fused silica inconel-coated beam splitter (Esco Products). The two beams are recombined on an identical fused silica inconel-coated beam combiner so that the beams are vertically displaced equally above and below the original beam height.

The pump, sample, and reference beams are made parallel and are focused into the flow cell with either a 15 cm focal length plano-convex lens or a 20 cm focal length 90° off-axis aluminum paraboloidal mirror. The beams have parallel polarization. Only the pump and sample beams are allowed to overlap spatially in the flow cell, as determined by alignment through a small pinhole. The two probe beams (sample and reference) are then spatially separated from the pump beam and recollimated. Baffles are used to eliminate fluorescence due to the pump beam alone. Both sample and reference beams are focused into a $^1/_8$ m monochromator with a 0.3 mm entrance slit (CVI Laser CM110SP) using a 3 cm focal length achromat. For time-resolved studies the exit slit is usually set to 8 nm band-pass. For measurement of the pump or probe spectrum a 0.5 nm band-pass was used.

The sample and reference beams are recollimated after exiting the monochromator, separated, and focused onto 400 MHz UV-enhanced silicon photodiodes (Thor Labs DET 210). The photodiode outputs are then amplified as necessary (Mini Circuits ZFL 500LN) and fed into two boxcar integrators (Stanford Research Systems SRS 250). The outputs of the sample and reference boxcars are digitized to 16 bit precision with a data acquisition board (National Instruments Lab 1200PC) controlled by in-house written Labview software running on a Pentium-based microcomputer. The sample signal is divided by the reference signal on a shot-to-shot basis in order to remove intensity and sample fluctuations. Using the dual beam geometry the noise level is ∼1 mOD. The signal-to-noise ratio is improved by extensive averaging.

To obtain the instrument response function the flow cell is replaced by a 1 mm fused silica cuvette containing neat toluene or a toluene/naphthalene solution. The pump beam is sufficiently intense to create a Kerr lens in the solution, which refracts the sample beam away from the detector for the duration of the pump pulse. This technique is useful in the UV and with continuum probe schemes, where standard cross correlation techniques relying on second harmonic generation are difficult and inefficient. The chirp is approximately 4 fs/nm and is taken into account in the data analysis where indicated.

Two modes of data collection were employed. For the determination of decay constants, the spectrometer was set at a fixed wavelength and the translation stage was driven with a

linear step size, typically 100 fs/step. The sample signal was ratioed to the reference signal to normalize the signal to fluctuations in the laser intensity and sample cell changes. The data were converted to transient absorbance by $\Delta A = \log(I_0/I(t))$, where $I(t)$ is the normalized signal and I_0 is obtained by averaging the normalized signal obtained before the photolysis pulse, $I(t<0)$ (the baseline).

Frequency-resolved transient absorption spectra were obtained by scanning the monochromator linearly with respect to wavelength at selected time delays. The time base for these experiments was increased in a logarithmic fashion rather than linearly in order to reduce the overall acquisition time. A preflash baseline was obtained by sampling the transmission of the sample and reference beams at several time delays less than t_0. These traces were averaged together to obtain a baseline transmission of the spectrometer. The change in absorbance was calculated by $\Delta A = \log(I_{sample}(\lambda,t)/I_{ref}(\lambda)) - \log(I_{sample}(\lambda,t<0)/I_{ref}(\lambda))$, where $I_{ref}(\lambda)$ indicates that the reference beam does not overlap the pump beam. Any fluorescence due to the pump beam alone was removed by this procedure.

Materials. FAD (98% purity) was obtained from Sigma and dissolved in HPLC grade water to a working concentration of 0.1−1 mM. No discernible difference in the dynamics was observed over this concentration range. FMN (riboflavin 5′-phosphate) was obtained from Lancaster in 96% purity and from Sigma in ∼70% purity. The impurities consist of riboflavin, riboflavin 4′-phosphate, and riboflavin 3′-phosphate but produced no obvious difference in the measured dynamics. These flavins are similar to FMN (riboflavin 5′-phosphate) in that they all lack a tethered adenine. Caffeine (Aldrich) was used at 50 mM concentration. Measurements were made at room temperature. No effort was made to deoxygenate the samples. Sample integrity was monitored by measuring the absorption spectrum before and after laser photolysis on a UV/vis diode array spectrometer (HP 8452). The samples were handled under yellow lights to avoid unnecessary photoreactions.

Data Analysis. Each data set includes a cross correlation measurement at 0.05 ps, resolution as described above. The cross correlation was fit to a Gaussian function. Typical values for the cross correlation were $\sigma = 175$ fs. This corresponds to a full width at half-maximum of about 410 fs. The Gaussian parameters were used to generate a noiseless instrument response function. This was used with a "convolute-and-compare" technique to fit a multiexponential model function to the experimental data. Minimization was performed using a simplex algorithm (MATLAB 5.3, The Mathworks).[24] The free parameters in the fit are the lifetimes of the exponential model functions and the zero of time for the cross correlation. The amplitudes were calculated by a linear least squares procedure rather than by allowing them to be free parameters of the fit.

For the frequency-resolved transient absorption experiments, singular value decomposition (SVD) was employed to remove uncorrelated noise between spectra obtained at different time delays. The SVD procedure operates on a data matrix **A**, whose rows and columns correspond to ΔA in time and wavelength respectively, returning three matrices, **U**, **S**, and **V**, such that $\mathbf{A} = \mathbf{USV}^T$. SVD decomposes the data matrix (**A**) into a set of orthogonal basis vectors (the **U** matrix) that represent the information content of the data.[25−27] A set of weighting coefficients, the diagonal matrix **S**, is also obtained. Typically, the weighting coefficients fall off rapidly with only the first few elements having significant value. At the same time, the basis vectors go from being highly structured to random. Examination of the basis vectors and their corresponding **S** coefficients allows for a rational truncation of the **S** matrix, $\mathbf{S}^i_{trunc}$, where $\mathbf{S}^i_{trunc}/\mathrm{Tr}(\mathbf{S}) > 0.05$ was used as a cutoff. The smoothed data matrix $\mathbf{A}_s$ is reconstructed by $\mathbf{A}_s = \mathbf{US}_{trunc}\mathbf{V}^T$.

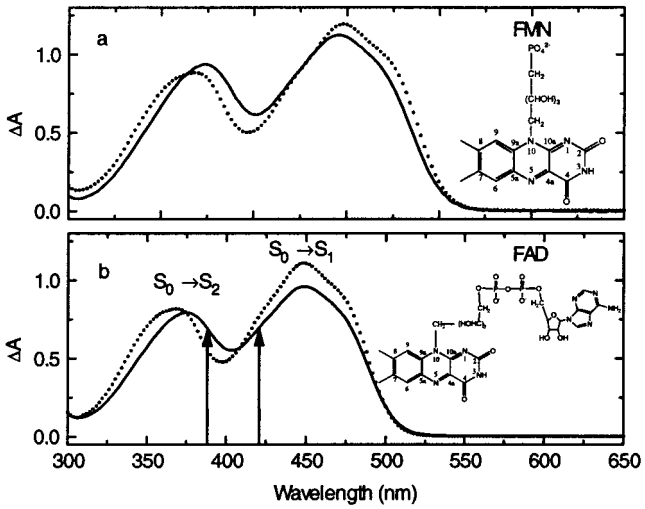

Figure 1. (a) Absorption spectrum of FMN in water (—) and formamide (●). (b) Absorption spectrum of FAD in water (—) and formamide (●). The spectra were obtained in a 1 cm path length quartz cuvette at 100 μm concentration at room temperature. The arrows indicate the excitation wavelength range used for the study.

Results

Parts a and b of Figure 1 show the absorption spectra for FMN and FAD taken at 100 μM in H_2O (solid line) and formamide (dots) with a path length of 1 cm. The structures of FAD and FMN are also indicated on the figure for reference. The two flavins have nearly identical spectra in the two different solvents. The arrows indicate the pump tuning range used in these experiments. This range allowed for red-edge excitation of the $S_0 \rightarrow S_2$ transition and blue-edge excitation of the $S_0 \rightarrow S_1$ transition. In general, it is assumed that both transitions are excited to various degrees throughout this tuning range. Excitation below about 400 nm resulted primarily in population of the S_2 state (but see below), while above 400 nm S_1 is preferentially populated. This assignment is in agreement with low-temperature Stark spectroscopy studies on flavins, which has been useful in assigning the two overlapping electronic transitions.[28]

Transient Spectra Studies. Transient absorption spectra for FMN and FAD (250 μM) in water were obtained for the $S_0 \rightarrow S_2$ transition at roughly 2, 10, and 100 ps after excitation with 389 nm light (Figure 2a,b). A white light continuum, generated from the Ti:S amplifier fundamental, was used as a probe. The continuum had useful intensity above about 410 nm. It was not possible to probe below this wavelength using a continuum generated from the fundamental of the amplifier; therefore the ground-state bleach resulting from the $S_0 \rightarrow S_2$ transition was not obtained.

Immediately evident from these data is the difference in the rate of decay of the transient absorption signal between the two molecules. FMN does not decay appreciably within the 100 ps time window, while excited FAD has decayed substantially between 1.6 and 10 ps. Modest decay of the FAD transient is observed between 10 and 100 ps. The primary result from these data is that adenine quenches excited-state flavin in FAD in less than 10 ps; time-resolved data presented below demonstrate that this reaction takes place in less than 5 ps.

With the exception of this ultrafast excited-state quenching, which is a new result, the observed spectral evolution from 10

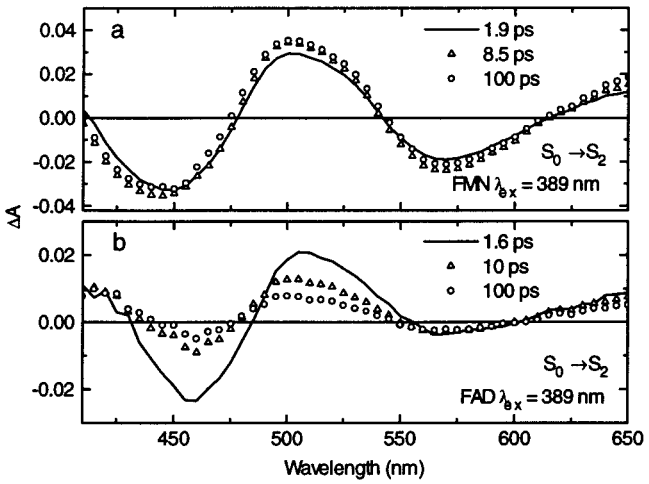

Figure 2. (a) Transient spectra of 250 μM FMN in water taken with 389 nm excitation, at 1.9 ps (—), 8.5 ps (△), and 100 ps (○) after excitation. (b) Transient spectra of 250 μM FAD in water taken with 389 nm excitation, at 1.6 ps (—), 10 ps (△), and 100 ps (○) after excitation.

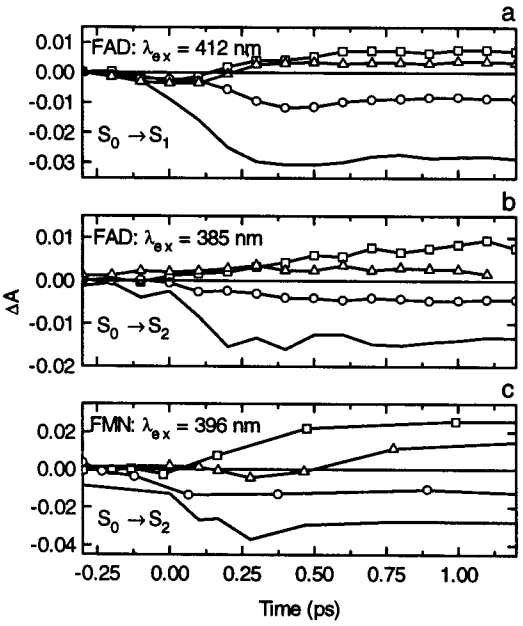

Figure 3. (a) Time-resolved decays of FAD in H_2O less than 1.2 ps after excitation at 412 nm with 8 nm band-pass using a linear time base of 0.1 ps/step. Probe wavelengths are (—) 430 nm, (△) 510 nm, (○) 570 nm, and (□) 650 nm. (b) Time-resolved decays of FAD in H_2O less than 1.2 ps after excitation at 385 nm with 8 nm band-pass using a linear time base of 0.1 ps/step. Probe wavelengths are (—) 430 nm, (△) 510 nm, (○) 570 nm, and (□) 650 nm. (c) Time-resolved decays of FMN in H_2O less than 1.2 ps after excitation at 396 nm with 8 nm band-pass using a logarithmic time base. Probe wavelengths are (—) 440 nm, (△) 510 nm, (○) 570 nm, and (□) 650 nm. All these data have been corrected for dispersion by using the Kerr effect cross correlation collected with each data set (cross correlation not shown).

to 100 ps agree well with that obtained by other workers.[8,12,29] The negative absorption in the 450 nm region is ascribed to ground-state bleaching for the $S_0 \rightarrow S_1$ transition. In the case of FAD, this bleach is filled in partially within about 10 ps. The increased absorption peaked at about 505 nm is thought to be an excited-state absorption (ESA, $S_1 \rightarrow S_n$). Evidence for this supposition is presented below. The negative absorption at 560 nm is ascribed to stimulated emission since flavins have a strong fluorescence emission band in this region. A second ESA band is observed growing in beyond 600 nm.

The transient spectra of both species within the first picosecond is shown in Figure 3a−c. These data are corrected for the chirp of the white light continuum. When FAD (Figure 3a) is excited primarily into the S_1 manifold (λ_{ex} = 412 nm) a ground-state bleach at 430 nm is observed within the instrument response time (solid line).[30] The stimulated emission at 570 nm (open circles) does not develop fully until about 250 fs after the photolysis pulse, though an accurate decay time for this process is difficult to obtain with 400 fs time resolution. Since excitation is primarily into the blue edge of S_1 vibrational relaxation is expected to occur before the stimulated emission develops. This is expected in the case of flavins because the Stokes shift for the $S_1 \rightarrow S_0$ transition is large (~3000 cm^{-1}). Thus, it appears that intramolecular vibrational relaxation takes place in about 250 fs. Another possible relaxation route is intermolecular vibrational relaxation due to solvent interactions. Experiments in different solvents might help to resolve this question. Positive absorption features at 510 nm (open squares) and 650 nm (open triangles) are coincident with the 570 nm stimulated emission. This suggests that these features are excited-state absorption transitions originating from the S_1 manifold.

Figure 3b shows the results for 385 nm excitation of FAD in water (S_2 manifold). These data give new information on the rate of internal conversion from S_2 to S_1, which had been addressed indirectly until now. The decays look very similar to the S_1 excitation experiments within the signal-to-noise. This indicates that internal conversion from $S_2 \rightarrow S_1$ takes place in less than about 100 fs. Internal conversion rates of this magnitude are expected for large molecules such as flavins,[31] and a simple calculation based on the energy gap law[32] is in agreement with this result.

The short time dynamics of FMN excited primarily into the S_2 state are shown in Figure 3c (396 nm excitation). This scan was obtained with a logarithmic time base (the ground-state bleach is shown at λ_{ex} = 440 nm). Even though the time step is more coarse than the linear time base used to obtain Figure 3a,b the similarity between the FMN and FAD decays is striking. This result suggests that the mechanism responsible for quenching operates on a slower time scale than that for either internal conversion or vibrational relaxation, since FMN does not undergo quenching because it lacks the adenine moiety.

Time-Resolved Decays. To make a more quantitative measurement of the quenching rate in FAD, time-resolved decays were performed at 0.1 ps/step at selected pump and probe wavelengths over a longer time base. One-color pump probe decays of FAD in H_2O at 393, 407, and 418 nm are shown in Figure 4. The scan range was 30 ps at 0.1 ps/step. The transient decays have not been normalized to either the pump pulse energy or the absorbance of the sample at the excitation wavelengths; therefore the amplitudes of the absorbance changes should be compared only on a relative basis. A typical instrument response function is shown for reference (●).

Regardless of the excitation wavelength, the signal decays to a steady-state value within about 25 ps. Significant amplitude continues out to beyond 1 ns without appreciable decay (data not shown). Excitation below ~410 nm results in an increase in absorption. At shorter wavelengths this increase is rise time-limited, while at longer wavelengths the rise time is longer than the instrument response function. An increase in absorption is still observed at the shortest excitation wavelength employed (385 nm, data not shown), indicating that the excited state bleach extends broadly below this technical limit. Since internal conversion is very fast (see above) this ESA most probably

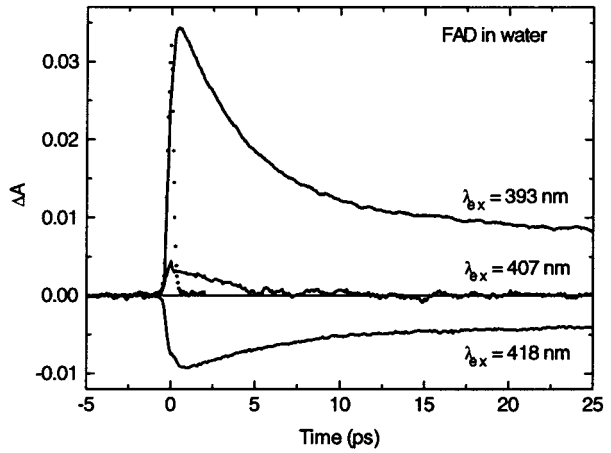

Figure 4. Time-resolved decays obtained as a function of excitation wavelength for 1 mM FAD in water at 0.1 ps/step. Photolysis was carried out at different pump energies for the different wavelengths so that ΔA was not directly comparable between the different excitation wavelengths. Excitation wavelengths below 400 nm correspond to red-edge excitation of the S_2 state, and wavelengths above 410 nm correspond to blue-edge excitation of the S_1 state. Maximum photolysis is $\Delta A/A \sim 5\%$ at $t = 0$ for 393 nm. The dotted line at $t = 0$ is the instrument response function.

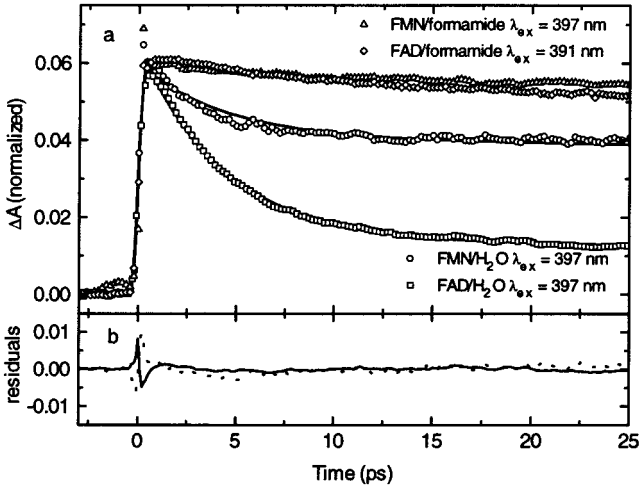

Figure 5. (a) Effect of solvent on the π-stacking of adenine with isoalloxazine. Single wavelength decays for 1 mM FMN (○) and FAD (□) in H_2O, along with biexponential model fits (—), and 1 mM FMN (△) and FAD (◇) in formamide taken at the indicated excitation wavelengths. The data have been normalized to the same peak amplitude for comparison. (b) Residuals from the biexponential fit to the decay data in water (see text for details).

arises from absorption of a 385 nm probe photon (~26 000 cm^{-1}) from the S_1 manifold (450 nm; ~22 222 cm^{-1}), leading to a transition to the S_4 state (~207 nm), which has several times the oscillator strength of the 450 nm transition.

From about 410 to 490 nm a decrease in absorption is observed (see Figure 2). For these decays, a fast (subpicosecond) component is observed as well as a very fast transient, as seen on the rising edge of the 418 nm transient in Figure 4. The amplitude of this sharp feature is linear with the pump power (data not shown) and is present in the solvents alone. This subpicosecond component is probably due to the formation of a Kerr lens in the solvent due to the pump beam.[33]

The transient absorption decays of solutions of FAD and FMN at 397 nm in water and formamide are shown in Figure 5a. The scan range was 30 ps at 0.1 ps/step. Quenching of the excited state of FAD in aqueous solution (□) is evident from the decrease in amplitude of the signal that occurs within about 4 ps. For both flavins in aqueous solution there is a much longer-lived component that contains significant amplitude, especially in the case of FMN (○). Formamide was used as a solvent in order to substantiate the origin of the picosecond quenching. It is known that formamide breaks up stacking interactions between isoalloxazine and adenine in FAD because the adenine moiety is more effectively solvated by this solvent.[34] Both FAD (—) and FMN (△) in formamide show virtually no excited state decay when compared with the decays taken in water. In addition, the decays in formamide are nearly identical, as contrasted with the dramatic difference between FMN and FAD in water.

TABLE 1: Lifetime and Relative Amplitudes of Biexponential Quenching Model

molecule	λ (nm)*	τ_1 (ps)	τ_2 (ps)	a_1 (rel %)	a_2 (rel %)
FMN/H_2O	396	4.6 (0.2)	429 (82)	29 (1)	71 (1)
FMN/H_2O	387	5.1 (0.2)	297 (24)	20 (1)	80 (1)
FMN/H_2O	391[a]	3.9 (0.5)	462 (77)	25 (6)	75 (6)
FAD/H_2O	397	4.6 (0.2)	429 (82)	76 (1)	24 (1)
FAD/H_2O	391	3.7 (0.2)	228 (15)	52 (1)	48 (1)
FAD/H_2O	383	5.1 (0.2)	297 (24)	53 (1)	47 (1)
FAD/form	391	3.7 (0.2)	228 (15)	8 (2)	92 (2)
FAD/form	383	3.9 (0.1)	132 (2)	7 (2)	93 (2)
FMN/form	397	7.9 (0.7)	1482 (1116)	13 (66)	87 (12)
FMN/H_2O/caffeine	391[b]	3.9 (0.5)	462 (77)	55 (13)	45 (13)

[a] Single color studies. [b] Average of 387 and 396 nm excitation data sets.

We take a simplified approach in analyzing these data because we wish to isolate and compare the amplitude of the quenching reaction with the amplitude corresponding to those molecules that do not undergo quenching. To compare the amplitudes of the short and long-lived components, we have fitted the data to a biexponential model function, as indicated by the solid lines. The residuals to these fits are plotted in Figure 5b. The large deviation around $t = 0$ ps indicates that a biexponential model function is an inadequate representation for the observed dynamics. In part, this is due to the 25 ps time window, which limits our ability to define time constants that are 4−5 times longer than this range; the decay of the long-lived components are not resolved in 30 ps despite the relatively high signal-to-noise ratio. However, the model is sufficient for the semiquantitative nature of the analysis as discussed below. It is worth noting that the biexponential model function fails completely when $\lambda_{ex} > 410$ nm because of the presence of an additional fast component in the rise of the signal (data not shown).

Fitting to the biexponential model function was performed using a decay from FAD and FMN taken at the same pump and probe wavelengths which were then fitted simultaneously. Several such pairs from different runs and samples were used to obtain an average and deviation. The results for excitation from 383 and 397 nm are compiled in Table 1. Given the semiquantitative nature of our approach we average the results from these two excitation wavelengths. FAD in water (1 mM) gives a 5 ps lifetime with about 65% relative amplitude. A longer time constant, roughly 350 ps, is obtained with about 35% relative amplitude. The amplitude of this long-lived component undoubtedly represents those FAD molecules that are unstacked, as well as those that undergo dynamic quenching within the time window of the experiment. In contrast, FMN in water (1 mM) has only about 25% amplitude for the fast component and 75% amplitude for the slow component. The fast component may represent self-quenching by preformed FMN dimers. Studies by Gibson et al.[35] set the dimerization constant for FMN in water at 10 mM. At 1 mM FMN, the dimer

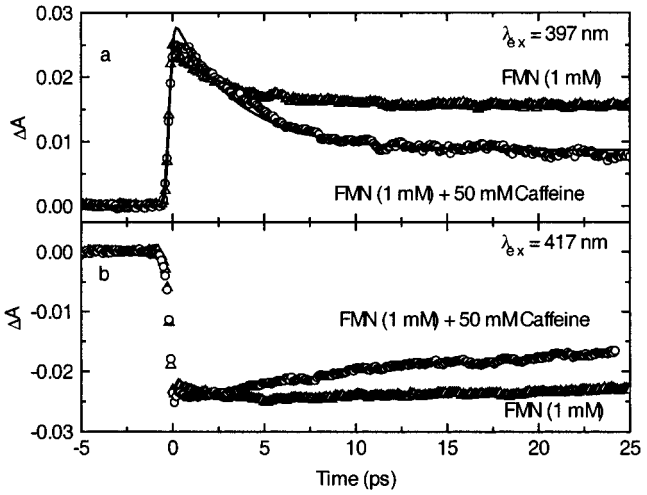

Figure 6. Excitation of the S_2 state of FMN (λ = 397 nm) without (△) and with (○) 50 mM caffeine. The decays are not scaled and can be compared directly. The biexponential fits are indicated by the solid lines. (b) As above for excitation into the S_1 state (λ = 418 nm). The structure at $t < 1$ ps is reproducible and may indicate ultrafast vibrational relaxation due to blue edge excitation of the state. These data are fit poorly by the biexponential mode function (fit not shown; see text).

fraction is about 8%. This may help explain the 25% amplitude for the fast decay component as the excited dimer would also undergo fast quenching.

The formamide solvent data were fitted to a biexponential model function to compare the ratio of fast to slow amplitudes. The results of the biexponential fitting are given in Table 1. The fast component is within a factor of 2 for these wavelengths, but the long component varies considerably, due to the lack of data to longer times. The relative amplitudes show the same trend as the water solvent experiments: in H_2O the relative amplitude is partitioned about equally between fast and slow components while in formamide less than 14% of the total amplitude is due to the fast component. It appears that formamide breaks up both the adenine/isoalloxazine complex in FAD and any FMN dimers that might also be contributing to ultrafast quenching. These results show that the quenching is due to stacking interactions in FAD and not electronic coupling of adenine and isoalloxazine through the ribtyl chain.

Finally, the excited-state dynamics of FMN and FMN with 50 mM caffeine are shown in Figure 6a,b for both 397 and 417 nm excitation. The decays for FMN in water were obtained first. The 1 mM FMN solution was subsequently caffeinated to 50 mM by the addition of solid caffeine and a new data set was obtained directly after. These data sets were fitted simultaneously as described above. Data sets for 387 and 396 nm excitation were averaged together. The results are presented in Table 1. Consistent with the FAD/FMN data, FMN in water has a 4 ps component with about 25% relative amplitude. This component rises to about 55% when caffeine is added to the solution. This value is lower than that achieved by FAD, but this is undoubtedly due to the lower concentration of FMN−caffeine complexes ($K_D = 1.1 \times 10^4$ M) relative to the flavin−adenine complex in the FAD solution.[5]

Discussion

We have obtained data that touch upon several aspects of excited-state dynamics in flavins. The most straightforward result we have obtained is a measurement of the time scale for quenching of the lowest singlet excited state of oxidized flavins by purines. The second result bears on the spectral evolution of the excited states. We begin with a discussion of the spectroscopy data and conclude with the excited-state quenching observation.

Excited-State Spectral Dynamics of Flavins. The motivation for understanding the spectral evolution of flavins goes beyond the intrinsically interesting photochemistry and physics of a complex heterocyclic molecule. Flavins are important biological redox cofactors whose electronic structure is exploited fully by nature. A complete knowledge of the spectral evolution of the excited state is essential for understanding the mechanisms of those flavoproteins that require light for catalysis (i.e., photolyases,[36] cryptochromes[37,38]). However, as has been shown by many workers, the flavoprotein function may also be influenced by flavin motion in the binding site[17,39] and also perhaps flavin structure (planarity).[18,40,41] Spectroscopy provides important data on these aspects of function. An additional motivation comes from the electronic interaction of flavin cofactors with aromatic residues in the cofactor binding site.[12,13,42−44] These interactions can lead to charge-transfer character that might modulate flavin redox activity.

Picosecond absorption spectroscopy has been useful in identifying possible intermediates in flavoenzyme−substrate charge-transfer complexes, as well as flavin−amino acid interactions that might affect catalysis. The work of Karen et al.[8] is an example. Using 25 ps pulses at 355 nm excitation, they found that excited-state oxidized flavin interacting with tyrosine in Riboflavin Binding Protein undergoes ultrafast relaxation in less than 33 ps to form a charge transfer state. Different behavior was observed in flavodoxin, where a flavin−tryptophan exciplex was thought to have formed within 33 ps of excitation but had a lifetime of several nanoseconds. The transient spectra and lifetimes for model complexes (flavin−indole and flavin−phenol) were found to be very sensitive to solvent.[12] The ability of the quencher to hydrogen bond to flavin also had a significant effect on the excited state dynamics, generally accelerating the quenching of the excited state.

To our knowledge, previous picosecond transient absorption studies of oxidized flavins have all employed excitation at 355 nm. This results in blue edge excitation of the S_2 state, which has a Franck−Condon maximum at about 370 nm (for FAD in water, 25 °C). In the work of Karen et al., lumiflavin in chloroform and riboflavin tetrabutyrate were studied with a broadband probe from 490 to 800 nm.[8] The lifetime of the transient was around 6−7 ns. This corresponds well with fluorescence lifetime measurements of the S_1 state so that the observed transient spectra were assigned to $S_1 \rightarrow S_n$ transitions. A negative absorbance was measured at 520 nm, which was ascribed to stimulated emission from the S_1 state.

MacInnis and Kasha studied the transient absorption spectrum of lumiflavin in methanol with excitation at 355 nm and 30 ps resolution.[29] Their transient absorption spectrum 100 ps after photolysis extends from 420 to 740 nm. They observed a negative absorbance from 420 to 460 nm, which they assigned as a ground-state bleach of the S_1 state. An increase in absorbance was observed from about 490 to 525 nm, which was interpreted as an $S_1 \rightarrow S_n$ excited-state absorption. From 525 to 630 nm a negative absorbance was interpreted as stimulated emission. Above this wavelength a positive absorbance was interpreted as $S_1 \rightarrow S_n$ excited-state absorption. These results and interpretation agree with the previous study, given the differences between flavins and solvents. In both experiments, internal conversion from the $S_2 \rightarrow S_1$ state was assumed to occur in less than 25 ps, although no data were supplied to

support this suggestion. With the probe wavelengths available, transitions into S_3 and S_4 were both possible.

In this study, no excited state absorption is seen until internal conversion was completed (see Figure 3a−c), which strongly suggests that the observed ESA bands result from the absorption of a photon from excited molecules in the S_1 state, whether produced by internal conversion or direct excitation. Additionally, it can be seen from Figure 2 that the ESA features track the decay of the ground-state bleach and the stimulated emission for up to 100 ps. Longer time base scans out to 3 ns show that these ESA features continue to track the stimulated emission and the ground-state bleach (data not shown). On the basis of these kinetics it seems logical to conclude that all of the ESA bands observed originate from the S_1 manifold. For example, relaxation into the S_1 state would leave the flavin with about 20 408 cm^{-1} of energy (assuming the 0−0 band is around 490 nm). Absorption into the S_4 state at 47 620 cm^{-1} would require a photon around 367 nm. While we are not able to generate this wavelength, single color transient absorption data with excitation at 383 nm (data not shown) show an absorption increase larger than that obtained when using 390 nm pulses. This could be the $S_1 \rightarrow S_4$ excited-state absorption. Supporting evidence for the S_1 origin of the ESA bands comes from the 650 nm region. This spectral region might correspond to an excited-state absorption from $S_1 \rightarrow S_3$ (the $S_0 \rightarrow S_3$ transition is maximum around 260 nm).

Despite these correlations there are some remaining questions. The transient absorption feature at 510 nm in both flavins (see Figures 2 and 3) would signify excited-state absorption at 250 nm, where these flavins have a lower extinction coefficient (data not shown) relative to the peak extinction for these transitions. Although the extinction at 250 nm is still much greater than that at 490 nm, assigning the 510 nm absorption increase to an ESA would be at odds with the observation of stimulated emission at 570 nm. This is because excited-state absorption at this wavelength would correspond to an $S_1 \rightarrow S_3$ transition at the peak of the transition intensity for this band. This should predominate over stimulated emission from the much less intense $S_1 \rightarrow S_0$ transition. Thus, the nature of these long-lived ESA bands in the transient spectra is still incomplete. Interestingly, the absorption spectrum of the cationic form of oxidized flavin is peaked at 390 nm and is more than twice as intense as the absorption of the neutral at this wavelength.[45] Other workers have observed photoionization in fully reduced flavins by a sequential two-photon absorption mechanism,[46] and this mechanism may be operative in the case of the flavoquinone as well. However, there are currently no data to support this supposition. Experiments at different pH values may help resolve this issue.

Quenching Dynamics of Flavins Complexed with Purines. We have shown that the quenching of excited flavins interacting with other purines occurs in less than 5 ps. Until now, direct measurements of excited-state quenching of FAD and FMN−quencher complexes were available from time-correlated single photon counting measurements, made in the lowest $\pi \rightarrow \pi^*$ transition ($S_0 \rightarrow S_1$ at ∼450 nm), or from transient absorption measurements with excitation into the S_2 state.[12] These studies did not find the fast component we have measured due to inadequate time resolution.

Recently, time-resolved absorption measurements on reduced flavins and flavoproteins by Enescu et al. were performed.[18] These studies were conducted with excitation at 312 nm and a temporal resolution of 800 fs. A biexponential decay model was used to fit the data, yielding a 4 or 130 ps component (species dependent) and a 1 ns component. The authors make a note that stacking interactions may be the origin of the 4 ps component, but this was not demonstrated. Our experiments show conclusively that stacking interactions (or conversely the destruction of stacking interactions) are responsible for the ultrafast quenching observed in these and other studies. Additionally, as has been shown in this work and by others,[17,47] a biexponential decay model is inadequate, especially when excited-state quenching is important. A maximum entropy analysis of the time-resolved fluorescence from S_1 by Leenders et al. has shown that it is more profitable to model the fluorescence decay using a Gaussian distribution of decay rates centered about 30 ps, 500 ps, and 4.8 ns.[17] As noted, this will be especially useful when there is conformational heterogeneity.

As discussed above, the dynamic quenching of FAD in water has a rate constant of $(5.3\ ns)^{-1}$. Over the 100 ps range of the data presented here, dynamic stacking would not be a major component of the observed kinetics. However, there will be partially stacked molecules that can attain a quenching conformation within the time scale of the transient absorption experiment. This would ultimately lead to a range of lifetimes, probably Gaussian in distribution. In addition, that fraction of molecules that does not undergo quenching will contribute to the long time decay amplitude. Maximum entropy analysis should be extremely useful in diagnosing the degree of stacking in this time regime. Measurements made over a range of temperatures where the degree of stacking can be modulated should be revealing.

Transient absorption data such as those reported in this work will help test and refine this hypothesis by allowing data to be collected over a much broader range of pump and probe energies. We intend to use both global analytical[26,48] and maximum entropy[47] techniques with transient absorption spectroscopy in order to arrive at a deeper understanding of how flavoproteins exploit the electronic structure of flavins to promote biological redox chemistry.

Conclusions

We have obtained transient absorption spectra and time-resolved decays for oxidized flavins over a wide range of pump and probe wavelengths. We have measured the rate for quenching of flavins by adenine and caffeine to be about 4 ps. Additionally, we have obtained evidence that internal conversion from S_2 to S_1 electronic states proceeds in less than 100 fs and that vibrational relaxation in the S_1 manifold takes place in less than 500 fs.

Acknowledgment. We thank Drs. Marilyn Jorns, Frank Spano, and Michael Fayer for profitable discussions about flavins, time-resolved spectroscopy, and photophysics. In addition, the authors want to thank the reviewers for their critical reading of the manuscript, which has helped to clarify several of the reported observations.

References and Notes

(1) Müller, F. The Flavin Redox-System and Its Biological Function. In *Topics in Current Chemistry*; Springer-Verlag: Berlin, 1983; Vol. 108, pp 71−107.

(2) Ghisla, S.; Massey, V. *Eur. J. Biochem.* **1989**, *181*, 1−17.

(3) Stankovich, M. T. Redox Properties of Flavins and Flavoproteins. In *Chemistry and Biochemistry* of Flavoenzymes; Müller, F., Ed.; CRC Press: Boca Raton, FL, 1991; Vol. I.

(4) Walsh, C. *Acc. Chem. Res.* **1980**, *13*, 148−155.

(5) Weber, G. *Biochem. J.* **1950**, *47*, 114−121.

(6) Barrio, J. R.; Tolman, G. L.; Leonard, N. J.; Spencer, R. D.; Weber, G. *Proc. Natl. Acad. Sci. U.S.A.* **1973**, *70*, 941−943.

(7) McCormick, D. B. *Photochem. Photobiol.* **1977**, *26*, 169−182.

(8) Karen, A.; Sawada, M. T.; Tanaka, F.; Mataga, N. *Photochem. Photobiol.* **1987**, *45*, 49−53.
(9) Kainosho, M.; Kyogoku, Y. *Biochemistry* **1972**, *11*, 741−752.
(10) Kotowycz, G.; Teng, N.; Klein, M. P.; Calvin, M. *J. Biol. Chem.* **1969**, *244*, 5656−5662.
(11) Copeland, R. A.; Spiro, T. G. *J. Phys. Chem.* **1986**, *90*, 6648−54.
(12) Karen, A.; Ikeda, N.; Mataga, N.; Tanaka, F. *Photochem. Photobiol.* **1983**, *37*, 495−502.
(13) Breinlinger, E. C.; Rotello, V. M. *J. Am. Chem. Soc.* **1997**, *119*, 1165−1166.
(14) Scannell, M. P.; Fenick, D. J.; Yeh, S.-R.; Falvey, D. E. *J. Am. Chem. Soc.* **1997**, *119*, 1971−1977.
(15) Rehm, D.; Weller, A. *Isr. J. Chem.* **1970**, *8*, 259−271.
(16) Stanley, R. J.; Boxer, S. G. *J. Phys. Chem.* **1995**, *99*, 859−63.
(17) Leenders, R.; Van Hoek, A.; Van Iersel, M.; Veeger, C.; Visser, A. J. W. G. *Eur. J. Biochem.* **1993**, *218*, 977−84.
(18) Enescu, M.; Lindqvist, L.; Soep, B. *Photochem. Photobiol.* **1998**, *68*, 150−156.
(19) Mataga, N.; Chosrowjan, H.; Shibata, Y. *J. Phys. Chem. B* **1998**, *102*, 7081−7084.
(20) Visser, A. J. W. G.; van der Berg, P. A.; Visser, N. V.; van Hoek, A.; van den Burg, H. A.; Parsonage, D.; Claiborne, A. *J. Phys. Chem. B* **1998**, *102*, 10431−10439.
(21) van der Berg, P. A.; van Hoek, A.; Walentas, C. D.; Perham, R. N.; Visser, A. J. W. G. *Biophys. J.* **1998**, *74*, 2046−2058.
(22) Stanley, R. J.; Macfarlane, A. W., IV. Direct Measurements of Ultrafast Excited-State Quenching of Isoalloxazine by Adenine in FAD. *Proceedings of the 13th International Congress on Flavins and Flavoproteins*, 1999, Konstanz, Germany; Agency for Scientific Publications: Berlin, 1999.
(23) Fork, R. L.; Shank, C. V.; Hirlimann, C.; Yen, R.; Tomlinson, W. J. *Opt. Lett.* **1983**, *8*, 1−3.
(24) Lagarias, J. C.; Reeds, J. A.; Wright, M. H.; Wright, P. E. *SIAM J. Optimization* **1999**, *9*, 112−147.
(25) Lambright, D. G.; Balasubramanian, S.; Boxer, S. G. *Chem. Phys.* **1991**, *158*, 249−60.
(26) Hofrichter, J.; Henry, E. R.; Sommer, J. H.; Deutsch, R.; Ikedo-Saito, M.; Yonetani, T.; Eaton, W. A. *Biochemistry* **1985**, *24*, 2667−2679.
(27) van Holde, K. E.; Johnson, W. C.; Ho, P. S. *Principles of Physical Biochemistry*; Prentice Hall: Upper Saddle River, NJ, 1998.
(28) Stanley, R. J.; Jang, H. *J. Phys. Chem. B* **1999**, *103*, 8976−8984.
(29) MacInnis, J. M.; Kasha, M. *Chem. Phys. Lett.* **1988**, *151*, 375−8.
(30) A large negative dip was observed at zero time for all transient decays when $\omega_{ex} - \omega_{probe} \approx 3180$ cm^{-1} in water. For $\lambda_{ex} = 390$ nm this corresponds to a dip in the transient absorptoin spectrum at about 450 nm. This was found to be stimulated Raman scattering due to the *solvent* only. This interpretation was demonstrated by setting the excitation wavelength of a fluorometer to the laser excitation wavelengths and measuring the Raman scattering from a cuvette of the appropriate solvent. The width of the stimulated Raman line was limited by the monochromator band-pass. Therefore, the data showing the ground state bleach are selected slightly off the maximum of the absorption spectrum (450 nm) in order to avoid confusion over this large artifact. A similar feature was observed for data collected in formamide.
(31) Elsaesser, T.; Kaiser, W. *Annu. Rev. Phys. Chem.* **1991**, *42*, 83−107.
(32) Turro, N. J. *Modern Molecular photochemistry*; University Science Books: Mill Valley, CA, 1991.
(33) Boyd, R. W. *Nonlinear Optics*; Academic Press: San Diego, 1992.
(34) Miles, D. W.; Urry, D. W. *Biochemsitry* **1968**, *7*, 27912799.
(35) Gibson, Q. H.; Massey, V.; Atherton, N. M. *Biochem. J.* **1962**, *85*, 369−383.
(36) Sancar, A. *Biochemistry* **1994**, *33*, 2−9.
(37) Lin, C.; Ahmad, M.; Gordon, D.; Cashmore, A. R. *Proc. Natl. Acad. Sci. U.S.A.* **1995**, *92*, 8423−27.
(38) Hsu, D. S.; Zhao, X.; Zhao, S.; Kazantsev, A.; Wang, R.-P.; Todo, T.; Wei, Y.-F.; Sancar, A. *Biochemistry* **1996**, *35*, 13871−13877.
(39) Bastiaens, P. I. H.; Van Hoek, A.; Wolkers, W. F.; Brochon, J. C.; Visser, A. J. W. G. *Biochemistry* **1992**, *31*, 7050−60.
(40) Palfey, B. A.; Ballou, D. P.; Massey, V. *Biochemistry* **1997**, *36*, 15713−15723.
(41) Hasford, J. J.; Kemnitzer, W.; Rizzo, C. J. *J. Org. Chem.* **1997**, *62*, 5244−5245.
(42) Leenders, H. R. M.; Vervoort, J.; Van Hoek, A.; Visser, A. J. W. G. *Eur. Biophys. J.* **1990**, *18*, 43−55.
(43) Li, Y. F. **1992**, 5079.
(44) Zhou, Z.; Swenson, R. P. *Biochemistry* **1996**, *35*, 15980−15988.
(45) Müller, F. Free Flavins: Syntheses, Chemical and Physical Properties. In *Chemistry and Biochemistry of Flavoenzymes*; Müller, F., Ed.; CRC Press: Boca Raton, FL, 1991; Vol. I, pp 1−72.
(46) El Hanine-Lmoumene, C.; Lindqvist, L. *Photochem. Photobiol.* **1997**, *66*, 591−595.
(47) Leenders, R.; Kooijman, M.; Van Hoek, A.; Veeger, C.; Visser, A. J. W. G. *Eur. J. Biochem.* **1993**, *211*, 37−45.
(48) Lambright, D. G.; Balasubramanian, S.; Boxer, S. G. *Biochemistry* **1993**, *32*, 10116−24.